# Phase-field simulation of dendrite growth in Al-Si alloys under the action of forced convection and pressure

## Jia-qi Pei<sup>1</sup>, Wei-peng Chen<sup>1</sup>, Hua Hou<sup>1,2</sup>, and \*Yu-hong Zhao<sup>1,3,4</sup>

 School of Materials Science and Engineering, Collaborative Innovation Center of Ministry of Education and Shanxi Province for High-performance Al/Mg Alloy Materials, North University of China, Taiyuan 030051, P R China;
 School of Materials Science and Engineering, Taiyuan University of Science and Technology, Taiyuan 030024, P R China;
 Beijing Advanced Innovation Center for Materials Genome Engineering, University of Science and Technology Beijing, Beijing 100083, P R China;
 Institute of Materials Intelligent Technology, Liaoning Academy of Materials, Shenyang 110004, P R China

\*Corresponding address: e-mail: zhaoyuhong@nuc.edu.cn

Abstract: This study constructs a phase-field lattice-Boltzmann model that integrates forced convection and pressure, aiming to precisely regulate the microstructure of Al-Si alloy and enhance their casting performance. We systematically analyzed the influence mechanisms of forced convection and pressure on dendrite growth. Through simulations of the two-dimensional dendrite growth of Al-Si alloy under non-isothermal solidification conditions, we found that forced convection leads to the overlap of the thermal and solute fields, causing an uneven distribution of both. Heat and solute are transferred from the counter-flow side to the co-flow side at the dendrite arm tip, accelerating the growth rate of the counter-flow side dendrite arm. Under the condition of applying higher pressure, the growth rate of dendrites significantly increases. The grain size shows an increasing trend, the dendrites become finer, and the secondary dendrite arms are more developed. Moreover, the increase in pressure promotes nucleation and expedites the solidification rate. Overall, the results of this study are expected to provide a solid theoretical basis for improving the performance of Al-Si alloy castings.

Keywords: Al-Si; Phase-field method; Solidification; Eutectic

### 1 Introduction

On account of their exceptional casting properties, Al-Si alloy are extensively employed in the production of lightweight components, with particular prominence in the automotive domain <sup>[1]</sup>. Al-Si alloy are characterized by outstanding casting performance, remarkable corrosion resistance, and comprehensive mechanical properties.

In the field of alloy solidification, optimizing the solidification structure and improving performance have always been important research directions that attract much attention. Studies have shown that the application of external fields such as ultrasound and electromagnetic oscillation can effectively promote the transformation of dendritic crystals to equiaxed crystals, and significantly inhibit elemental segregation at the same time, thereby achieving remarkable results in improving the solidification structure and enhancing mechanical properties <sup>[2,3]</sup>. Forced convection affects the solidification

microstructure by altering the solute and temperature distribution near the solid-liquid interface. Phase-field method has shown great potential in material design and mechanism interpretation [4-7]. Previously, we have conducted in-depth research on the refinement method of forced flow of  $\alpha$  -Al dendrites [8].

Extrusion casting technology has become the preferred process for manufacturing partitions due to its unique advantage of being able to produce castings with dense structure, excellent performance and precise molding <sup>[9]</sup>. During the extrusion casting process, pressure, as a key thermodynamic parameter determining the microstructure and mechanical properties, has a quantitative impact on dendrite behavior. Many scholars have devoted themselves to the simulation and research related to the dendrite growth of alloy solidification under pressure <sup>[10,11]</sup>. For instance, Pan Haowei <sup>[12]</sup> constructed a phase field model suitable for simulating dendrite growth during alloy solidification under pressure conditions based on the

state equation. This model fully considers the influence of pressure on the Gibbs free energy of the solid and liquid phases of the alloy, the diffusion coefficient of solutes, and the equilibrium distribution coefficient of solutes. Shang Shan et al. [13] deeply explored the effect of periodic pressure on the lateral branch branching mechanism.

Based on the above research background, an in-depth exploration of the influence of forced convection and pressure on the morphology, growth and distribution of dendrite structure is of crucial significance for precisely regulating the solidification structure of aluminum-silicon alloy and effectively improving the performance of aluminum-silicon alloy castings.

In this study, a phase-field-lattice Boltzmann model forced convection and pressure was coupling established to regulate the microstructure of Al-Si alloy and enhance its casting performance. The influence mechanisms of forced convection and pressure on dendrite growth were analyzed. Given the similarity of different aluminum-based alloy during solidification process, the results of this study can be extended to other aluminum-based multi-component alloy, providing valuable insights for optimizing the microstructure of aluminum-based multi-component alloy and improving their mechanical properties.

### 2 Method

### 2.1 Phase-field method

The growth process of  $\alpha$  -Al dendrites under non-isothermal solidification conditions was described using the quantitative phase field model [14-16]. The phase field order parameter is represented by  $\phi_{\alpha}$ . In the solid phase,  $\phi_{\alpha}=+1$ ; in the liquid phase,  $\phi_{\alpha}=-1$ , and within the diffusion interface,  $\phi_{\alpha}$  smoothly changes from -1 to +1.

$$a_{s}^{2}(\boldsymbol{n}) \left\{ \frac{1}{Le} + Mc_{0}[1 + (1 - k)U] \right\} \frac{\partial \phi_{\alpha}}{\partial t} = \nabla \cdot \left[ a_{s}^{2}(\boldsymbol{n}) \nabla \phi_{\alpha} \right] + \sum_{\eta = x, y} \frac{\partial}{\partial \eta} \left[ \left| \nabla \phi_{\alpha} \right|^{2} a_{s}(\boldsymbol{n}) \frac{\partial a_{s}(\boldsymbol{n})}{\partial (\partial \phi_{\alpha} / \partial \eta)} \right] + (1 - \phi_{\alpha}^{2}) \left[ \phi_{\alpha} - \lambda (1 - \phi_{\alpha}^{2}) (\widetilde{T} + Mc_{0}U) (1 + \dot{\xi}) \right]$$

where,  $\lambda$  represents the coupling parameter of time and space; M is the slope of the liquidus line.  $c_0$  is the initial solute concentration far from the solid/liquid

interface. k is the equilibrium solute partition coefficient. t is time.  $\xi=0.5\Delta x\beta$  is the noise term [17].  $\Delta x$  represents the spatial step size.  $\beta$  is a random number that is uniformly distributed within the range [-0.5, 0.5].  $Le=D_T/D_l$  is the Lewis number;  $D_T$  and  $D_l$  represent the thermal diffusivity and the liquid-phase solute diffusivity respectively. The anisotropic function is  $a_s(\mathbf{n})=1+\varepsilon_4cos[4(\varphi-\varphi_0)]$ ,  $\varphi\in[0,2\pi]$  is the spherical coordinate angles,  $\varphi_0$  is the orientation difference angle, and  $\varepsilon_4$  is the anisotropic strength of the crystal [18].  $\mathbf{n}=-\nabla\phi_\alpha/|\nabla\phi_\alpha|$  is the unit vector perpendicular to the solid-liquid interface.

The evolution equation of the dimensionless solute field order parameter U is

$$\begin{split} \left(\frac{1+k}{2} - \frac{1-k}{2}\phi\right)\frac{\partial U}{\partial t} &= \nabla \cdot \left[D\mathbf{q}(\phi)\nabla U - \vec{j}_{at}\right] \\ &+ \frac{1}{2}[1+(1-k)U]\frac{\partial \phi}{\partial t} \\ &- \frac{1}{2}\nu\left\{ \begin{bmatrix} 1+k-(1-k)\phi]\nabla U \\ -[1+(1-k)U]\nabla\phi \end{array} \right\} \end{split}$$
 where, the vector  $\mathbf{J}_{at} = -1/(2\sqrt{2})(1-kD_s/D_l)[1+V]$ 

where, the vector  $J_{at} = -1/(2\sqrt{2}) (1 - k D_s/D_l)[1 + (1 - k)U](\partial \phi_{\alpha}/\partial t)(\nabla \phi_{\alpha}/|\nabla \phi_{\alpha}|)$  represents the anti-trapping term;  $q(\phi_{\alpha})$  is the interpolation function.  $D_s$  is the solid-phase solute diffusion coefficient.  $D = D_l \tau_0/W_0^2$  is the dimensionless solute diffusion coefficient.  $\tau_0 = \alpha_2 \lambda W_0^2/D_l$  is the relaxation time.  $W_0 = d_0 \lambda/\alpha_1$  is the interface thickness.  $d_0 = \Gamma/\Delta T_0$  is the chemical capillary length.  $\Gamma$  is the Gibbs-Thomson coefficient. the constants  $\alpha_1 = 0.8839$  and  $\alpha_2 = 0.6267$ .  $\boldsymbol{v}$  is the dimensionless flow velocity.

### 2.2 Lattice-Boltzmann method

To simulate the movement of the liquid phase and its convection effect on the concentration evolution equation, we employed a lattice-Boltzmann method. The lattice-Boltzmann equation is given by [30,31],

$$f_{i}(\mathbf{r} + \mathbf{e}_{i}\Delta t, t + \Delta t) =$$

$$f_{i}(\mathbf{r}, t) - \frac{1}{\tau_{f}} \left[ f_{i}(\mathbf{r}, t) - f_{i}^{eq}(\mathbf{r}, t) \right] + F_{i}(\mathbf{r}, t)\Delta t$$
(3)

where  $f_i(\mathbf{r},t)$  is the particle distribution function,  $f_i^{eq}(\mathbf{r},t)$  is the equilibrium distribution function,  $\tau_f = 3\nu/(c_s^2\Delta t) + 0.5$  is the single relaxation time,  $\nu$  is the kinetic viscosity,  $c_s = \Delta x/\Delta t$  is the lattice velocity,  $\mathbf{e}_i$  is the discrete particle velocity. The density  $\rho_{LB}$  and flow velocity  $\mathbf{v}$  are given by,

$$\rho_{LB} = \sum_{i=0}^{Q-1} f_i(\mathbf{r}, t)$$
 (4)

$$\rho_{LB} \boldsymbol{v} = \sum_{i=0}^{Q-1} \boldsymbol{e}_i f_i(\boldsymbol{r}, t)$$
 (5)

where Q is the number of discrete velocities, Q = 9(D2Q9 model) for 2D simulations. The distribution function  $f_i^{eq}(\vec{r}, t)$  is expressed as,

$$f_i^{eq}(\mathbf{r},t) = w_i \rho_{LB} \begin{bmatrix} 1 + \frac{3(\mathbf{e}_i \cdot \mathbf{v})}{c_s^2} \\ + \frac{9(\mathbf{e}_i \cdot \mathbf{v})^2}{2c_s^4} - \frac{3\mathbf{v} \cdot \mathbf{v}}{2c_s^2} \end{bmatrix}$$
(6)

where  $w_i$  is the weight function. There are three types of weighting factors in the D2Q9 model, which depend on the distance to the corresponding neighbor and the model used. These weighting factors are as follows:  $w_0 = 4/9$ ,  $w_{1-4} = 1/9$  and  $w_{5-8} = 1/36$  in the D2Q9 model. The discrete external force  $F_i(\mathbf{r},t)$  in a second order accuracy is obtained by,

$$F_{i}(\mathbf{r},t) = w_{i}\rho_{LB} \begin{bmatrix} 3\frac{\mathbf{e}_{i} - \mathbf{v}}{c_{s}^{2}} \\ +9\frac{(\mathbf{e}_{i} \cdot \mathbf{v})\mathbf{e}_{i}}{2c_{s}^{4}} \end{bmatrix} \cdot F_{D}(\mathbf{r},t)$$
(7)

with

$$F_D(\mathbf{r},t) = \left(-\frac{2\rho_{LB}\nu h}{W_0^2}\right) \left(\frac{1-\phi}{2}\right)^2 \nu \tag{8}$$

where  $F_D(\mathbf{r},t)$  is the dissipative drag force, and h=2.757 is a constant.

#### 3 Results and discussion

### 3.1 Growth of a -Al dendrites

In the simulation of the growth of multi-granular crystals with different orientations, the orientation of each grain is specified by the pre-existing solid phase seeds. As the grains grow, very small volumes of liquid phase are added to the solid phase, and it is assumed that the orientation of this new increment in the solid phase is the same as the local crystal orientation of the grain.

The phase field distribution of the two-dimensional growth process of multiple grains of Al-Si alloy is shown in Fig. 1. As the solidification proceeds, the grain tips gradually grow, and main grain arms appear. Without mutual collisions, the influence between the grains is very small. Each grain grows freely in the direction not affected by the boundary, and its morphology is the same as that of the grain growth of a single grain. Then multiple grains start to contact each other, and grain collisions occur. The growth of the affected main grain arms will be inhibited, resulting in grain boundary curvature or cessation of growth. Finally, the main trunk of the grain and the secondary grain arms are well developed.

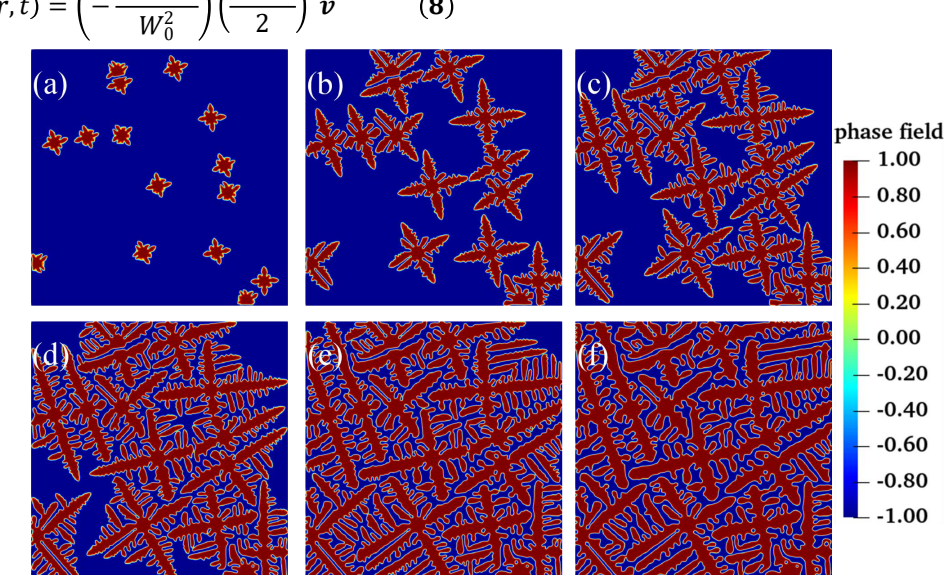


Fig. 1: Phase-field distribution of Al-Si alloy during dendrite growth (a) $t = 1000\Delta t$ , (b) $t = 3000\Delta t$ , (c) $t = 4500\Delta t$ , (d) $t = 6000\Delta t$ , (e) $t = 6000\Delta t$ , (f) $t = 6000\Delta t$ , (f)t = 6000 $9000\Delta t$ , (f)  $t = 15000\Delta t$ 

The distribution of Si solute field during the growth process of multiple dendrites in the Al-Si alloy is shown in Fig. 2. In the early stage of solidification, most grains

were not affected by the interaction of the solute fields. At  $t = 3000\Delta t$  (Fig. 2(b)), obvious collisions occurred between grains, and the solute fields of each dendrite were penetrated by the solute diffusion of other dendrites. The collisions were more intense, and the affected dendrite arms were restricted from growing. The phenomenon of solute enrichment occurred at the solid/liquid interface of the dendrites. The secondary dendrite region had a higher concentration because the dense dendrite area prevented the solute diffusion.

# 3.2 Comparison of dendrite under pure diffusion and forced convection

Fig.3 shows the comparison of the morphology of  $\alpha$ -Al dendrites during non-isothermal solidification of Al-Si alloy under pure diffusion and forced convection conditions. Under pure diffusion conditions, during the

initial stage of solidification, the nuclei are affected by quadruple anisotropy and exhibit a significant quasi-square shape. However, under forced convection, the grains no longer grow symmetrically and uniformly in all directions. Initially, due to the asymmetrical heat flux and solute flux acting on the arm of the dendrite, its growth direction tilts to the left. Forced convection promotes the growth of the reverse side of the dendrite, making the primary and secondary dendrites more developed. As the dendrites continue to grow, the heat and solute re-distributed during the solidification process will be carried to the downstream area by convection.

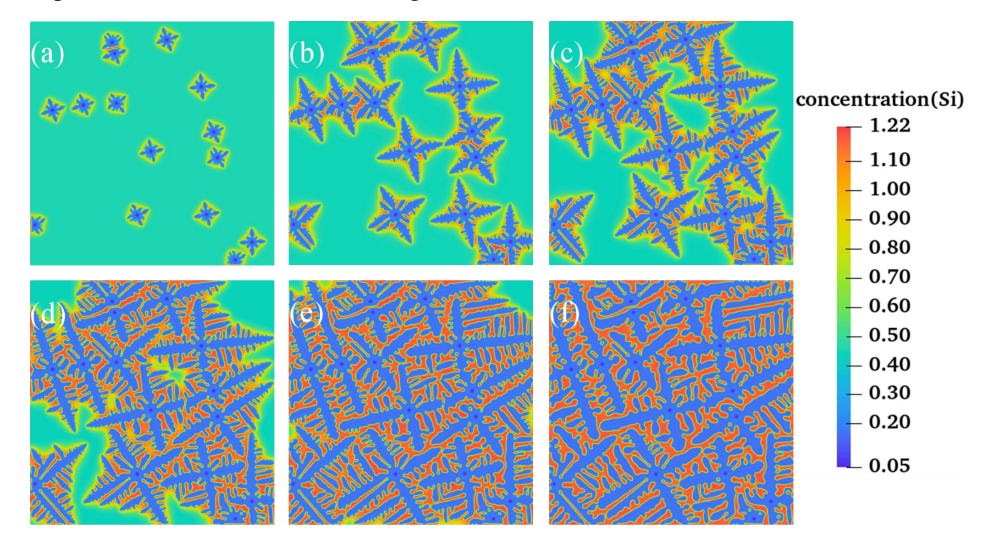


Fig. 2: Distribution of Si solute field during dendrite growth of Al-Si alloy (a)t =  $1000\Delta t$ , (b)t =  $3000\Delta t$ , (c)t =  $4500\Delta t$ , (d)t =  $6000\Delta t$ , (e)t =  $9000\Delta t$ , (f)t =  $15000\Delta t$ 

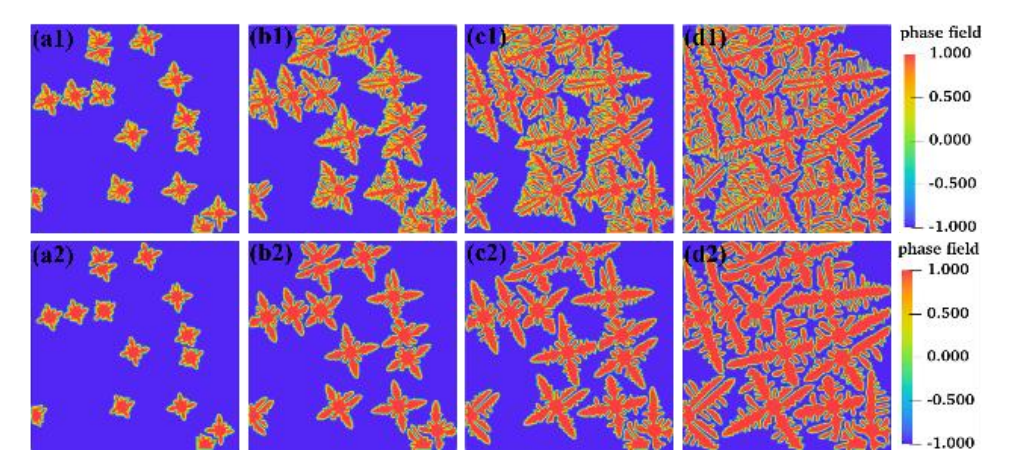


Fig. 3: Comparison of  $\alpha$ -Al dendrite morphology during non-isothermal solidification of Al-Si alloy under pure diffusion and forced convection (a)t =  $1000\Delta t$ , (b)t =  $2000\Delta t$ , (c)t =  $3000\Delta t$ , (d)t =  $5000\Delta t$ 

# 3.3 Comparison of dendrite under normal pressure and under pressurized conditions

The situation of solute segregation during the

non-isothermal solidification process of Al-Si alloy under different pressures is shown in Fig. 4. The increase in pressure significantly promoted nucleation and accelerated the solidification process. Compared with the temperature change, the improvement effect of pressure on the microstructure was more significant. With the continuous increase in pressure, the microstructure became finer and the sensitivity of the microstructure to temperature change decreased.

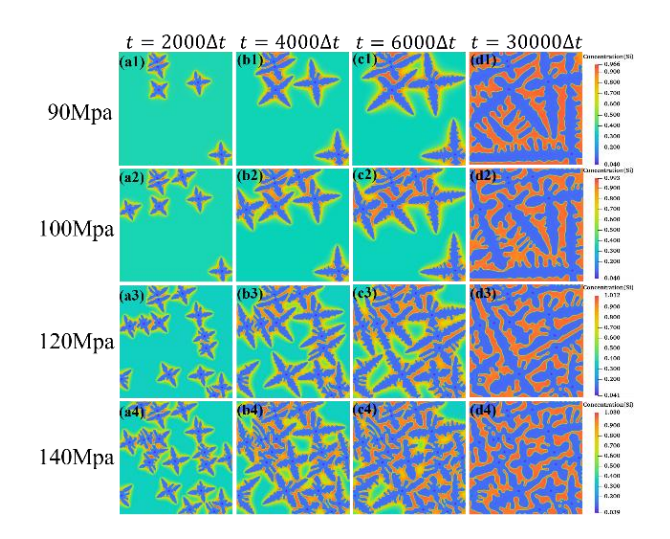


Fig. 4: Solute segregation during non-isothermal solidification of Al-Si alloy at different pressures

### 3.4 Comparison with Experimental Results

The simulation results were compared with the experimental ones. The microstructure diagram of Al-Si alloy after holding at  $530^{\circ}$ C for 2 hours and the comparison of Si solute distribution obtained from the phase field simulation are shown in Fig. 5. It can be observed that the  $\alpha$ -Al dendrites have coarse primary dendrite arms and developed secondary dendrite arms.

Due to the limitation of the simulation area and the mutual collisions among multiple dendrites, most dendrites exhibit asymmetry. These phenomena can be observed in both the simulation and experimental results, such as dendrite ① and ②. Due to the proximity of other dendrites near dendrite (1), obvious mutual collisions occurred between grains, and dendrite ① was more susceptible to the interaction of the solute field. The affected dendrite arms were restricted in growth and eventually became asymmetric dendrite morphology. Dendrite 2, due to the influence of fourfold anisotropy on the crystal nucleus during the initial solidification and the relatively small influence of the collision between dendrites later, showed a distinct quadrilateral-like morphology. The simulation results are in good agreement with the experimental results.

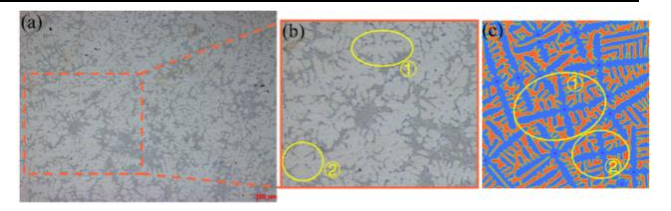


Fig. 5: (a) Metallographic microstructure of ZL118 alloy after holding at 530°C for 2 hours; (b) Enlarged view of the area indicated by the dotted line in (a). (c) Phase field simulation of Si solute distribution during the solidification process of Al-Si alloy

#### 4 Conclusions

- Simulated 2D/3D dendrite growth of Al-Si alloy under isothermal solidification, obtaining realistic dendrites with secondary or higher order arms.
- Observed lateral side-branch growth and solute segregation during dendrite growth.
- Under the influence of a larger flow velocity, more heat and solute are transported from the countercurrent side to the tip of the dendrite arm on the concurrent side, thereby accelerating the growth rate of the dendrite arm on the countercurrent side.
- Under the condition of applying higher pressure, the growth rate of dendrites significantly increases. Meanwhile, the grain size shows an increasing trend, the dendrites become finer, and the secondary dendrite arms are more developed. The increase in pressure promotes nucleation and accelerates solidification

### Acknowledgments

This research project was supported by the National Natural Science Foundation of China (Nos. 52074246, 52275390, 52375394), National Defense Basic Scientific Research Program of China (Nos. JCKY2020408B002), Key R&D Program of Shanxi Province (Nos.202102050201011).

### **Conflicts of interest:**

The authors declare that they have no known competing financial interests or personal relationships that could have appeared to influence the work reported in this paper.

### References

[1] Lasko Galina, Apel Markus, Carré, Antoine, et al. Effect of Microstructure and Hydrogen Pores on the Mechanical Behavior of an Al7%Si0.3%Mg Alloy

- Studied by a Combined Phase-Field and Micromechanical Approach[J]. Adv. Eng. Mater., 2012, 14, 236-247.
- [2] Ren Y, Ma W, Wei K, Yu W, Dai Y, Morita K, Degassing of aluminum alloy via the electromagnetic directional solidification, Vacuum, 2014, 109:82-85.
- [3] Zhang L, Han K, Man T, Wang E, Zuo X, Microstructural evolution and performance of in-situ Ag-Ni composite after Solidification under electromagnetic stirring and deformation, Journal of Iron and Steel Research, International, 2016, 23(7):638-646.
- [4] Xin T Z, Zhao Y H, Mahjoub R, et al. Ultrahigh specific strength in a magnesium alloy strengthened by spinodal decomposition[J]. Sci. Adv., 2021, 7, eabf3039.
- [5] Zhao Y H, Liu K X, Hou H, et al. Role of interfacial energy anisotropy in dendrite orientation in Al-Zn alloy: A phase field study[J]. Mater. Des., 2022, 216, 110555.
- [6] Zhao Y H. Editorial: Phase field method and integrated computing materials engineering[J]. Front. Mater, 2023, 10.
- [7] Zhao Y H, Xin T Z, Tang S, et al. Applications of unified phase-field methods to designing microstructures and mechanical properties of alloy[J]. MRS Bull., 2024, 49, 613-625.
- [8] Pei J Q, Chen W P, Zhang W D, et al. Phase field simulation for grain refinement in dendrite growth of A356 aluminum alloy [J]. J. Mater. Res. Technol., 2023, 27, 5615-5628.
- [9] Pei X L, Pei J Q, Hou H, et al. Optimizing casting process using a combination of small data machine learning and phase-field simulations[J]. npj Computational Materials, 2025, 11(1): 27.
- [10] Sawada T, Takemura K, Shigematsu K, et al. Dynamic pressure control for solution growth and its microgravity application. J Cryst Growth. 1996;158(3):328–335.

- [11] Koss M B, Lacombe J C, Chait A, et al. Pressure mediated effects on thermal dendrites. J Cryst Growth. 2005;279(1–2):170–185.
- [12] Pan H W, Han Z Q, Liu B C. Study on Dendritic Growth in Pressurized Solidification of Mg-Al Alloy Using Phase Field Simulation. Journal of Materials Science & Technology, 2016, 32(1): 68-75.
- [13] Shang S, Guo Z, Han Z Q. On the kinetics of dendritic sidebranching: A three dimensional phase field study [J]. Journal of Applied Physics, 2016, 119(16): 164305.
- [14] Ramirez J C, Beckermann C, Karma A, et al. Phase-field modeling of binary alloy solidification with coupled heat and solute diffusion[J]. Phys. Rev. E, 2004, 69(5), 051607.
- [15] Ohno M, Matsuura K. Quantitative phase-field modeling for dilute alloy solidification involving diffusion in the solid [J]. Phys Rev E: Stat. Phys., Plasmas, Fluids 2009, 79, 031603.
- [16] Guo Z P, Mi J, Grant P S. An implicit parallel multigrid computing scheme to solve coupled thermal-solute phase-field equations for dendrite evolution[J]. J Comput Phys, 2012, 231, 1781-96.
- [17] Ji K H, Dorari E, Clarke A J, et al. Microstructural pattern formation during far-from-equilibrium alloy solidification [J]. Physical Review Letters, 2023, 130(2): 026203.
- [18] Tourret D, Karma A. Growth competition of columnar dendritic grains: A phase-field study, Acta Materialia, 2015, 82, 64–83.
- [19] Takaki T, Sakane S, Ohno M, et al. Permeability prediction for flow normal to columnar solidification structures by large-scale simulations of phase–field and lattice Boltzmann methods[J]. Acta Materialia, 2019, 164: 237-249.
- [20] Zhang A, Guo Z P, Jiang B C, et al. Multiphase and multiphysics modeling of dendrite growth and gas porosity evolution during solidification[J]. Acta Materialia, 2021, 214: 117005.